Journal of Bio- and Tribo-Corrosion (2019) 5:103
https://doi.org/10.1007/s40735-019-0298-5

Theoretical and Experimental Investigation of the Synergistic Influence of Tricine and Iodide Ions on the Corrosion Control of Carbon Steel in Sulfuric Acid Electrolyte

M. M. EL-Rabiei[1] · H. Nady[1,2] · E. G. Zaki[3] · Mosaad Negem[1]

Received: 23 July 2019 / Revised: 31 August 2019 / Accepted: 3 October 2019 / Published online: 22 October 2019

Abstract
The combination of experimental and theoretical investigations of the adsorption/inhibition effect of tricine [*N*-(Tri(hydroxymethyl)methyl)glycine] as newly green corrosion inhibitor for the carbon steel has been investigated in aqueous H_2SO_4 electrolyte. The synergistic inhibition effect of tricine molecules and iodide ions on the corrosion of carbon steel in H_2SO_4 solution was scrutinized. Potentiodynamic polarization, electrochemical impedance spectroscopy, scanning electron microscope, and energy dispersive X-ray analysis techniques have been exploited to examine the influence of tricine and iodide on the corrosion of carbon steel in 0.1 M H_2SO_4 solution. SEM analysis shows the adsorbed layer inhibitors on carbon steel surface composed of tricine and iodide ions offering the long time protection for carbon steel in 0.1 M H_2SO_4 solution. Computational quantum and molecular dynamic simulation studies have been further used to calculate the electronic properties of tricine molecule to clarify the tricine molecular structure and inhibitive effect of the corrosion. Total energy (TE), E_{LUMO}, E_{HOMO}, dipole moment (D), energy gap (ΔE), softness (δ), and the change of the total energy (DET) have been calculated. The electrochemical and microstructure techniques display that the tricine is the greatly efficient inhibitor of mixed type with inhibition efficiency up to 87.4% and the adsorption of tricine adheres to Langmuir isotherm. The tricine inhibition efficiency increases via addition of iodide ions owing to synergistic effect.

Keywords Carbon steel · Tricine · Iodide · Polarization studies · Corrosion inhabitation · Acidic corrosion

1 Introduction

Metals, alloys, and metal matrix composites are the valuable materials for different applications like energy conversion, electrocatalysis, and industrial fields [1–4]. Carbon steel is the greatly essential material for the oil and gas industry and has a wide application in a broad spectrum of machinery despite its tendency to corrosion. The investigation of the corrosion behavior of carbon steel in several aqueous electrolytes has received a great attention. In such consideration, the corrosion inhibition of the carbon steel is very interesting. Most economical and practical method to mitigate electrochemical corrosion due to its low-priced and availability to fabricate easily various reaction vessels like cooling tower tanks and pipelines [5]. Acid solutions, especially H_2SO_4 and HCl, are broadly utilized in different industrial applications, such as petroleum industry, pickling of iron, chemical cleaning, and descaling of boilers.

One of the principal impediments to find an inhibitor which attains little or no impact on the environment attracted numerous researches in recent times [6]. Environmentally safe or green corrosion inhibitors are susceptible to be biodegradable and have no heavy metals or other poisonous compounds [7]. Tricine is an inhibitor with good inhibition efficiency, environmentally safe, and non-expensive and no report on tricine as corrosion inhibitor in the acidic environment has been reported. Quantum chemical calculations

✉ H. Nady
nhm00@fayoum.edu.eg

✉ Mosaad Negem
mra00@fayoum.edu.eg

[1] Chemistry Department, Faculty of Science, Fayoum Univer Sity, Fayoum, Egypt

[2] Chemistry Department, College of Science and Arts in Quryate, Jouf University, Al-Jawf, Kingdom of Saudi Arabia

[3] Egyptian Petroleum Research Institute, Nasr City, Cairo 11727, Egypt

were implemented to support the adsorption mechanism with the structure of tricine molecule. Recently, the research is interested to develop the green corrosion inhibitors, compounds with high inhibition efficiency but low risk to environment. The organic molecules containing different heteroatoms like nitrogen, oxygen, and sulfur atoms are effective inhibitors for H_2SO_4 corrosion. The inhibiting action of such compounds is ascribed to the adsorption of the molecules to the surface of metal and their strong chemical activity. The adsorbed inhibitor on carbon steel surface in acid environment leads typically to a reformation of the double layer structure with a reduction of the rate of anodic metal dissolution and the hydrogen ion cathodic reduction. Several studies are commenced to determine synergistic effects for some other additives such as anions. Interestingly, adding halide ions such as iodide ions into H_2SO_4 electrolyte which contains some organic compounds described to yield the necessitated enhancement [8, 9]. The choice of this inhibitor was based on the fact that tricine contains lone pairs of electrons on hetero-atoms such as N and O, which invoke the greater adsorption of the tricine inhibitor molecules on the carbon steel surface. In addition, some inorganic additives such as iodate, molybdate, and borate are used for corrosion inhibition for iron alloys in H_2SO_4 solutions [10].

The present work investigates the use of tricine (*N-(Tri(hydroxymethyl)methyl) glycine*) as corrosion inhibitor for carbon steel in 0.1 M H_2SO_4 electrolyte using electrochemical techniques. Potentiodynamic polarization and electrochemical spectroscopy of impedance (EIS) techniques have been utilized to determine the inhibition efficiency of the tricine inhibitor. The adsorption mechanism of the inhibitor was determined. Also, the synergistic effect of iodide ions on adsorption and corrosion-inhibitive characteristic of tricine molecules is investigated. The association between the efficiency of inhibition and molecular structure has been considered via molecular dynamics simulation (MD) and quantum chemical calculation.

2 Experimental

The working electrodes were made as massive rod from commercial grade carbon steel (grade 1030). For the electrochemical measurements, cylindrical carbon steel electrodes were mounted into epoxy resin inside Pyrex tubes by two-component epoxy resin leaving only 0.2 cm^2 of the surface area immersed into the corrosive electrolyte. The electrochemical cell used a three-electrode cell manufactured from Pyrex, with the saturated calomel in the role of reference electrode and the platinum counter electrode. Prior to each experiment, the working electrode was mechanically polished with a series of emery papers (from 400 to 2000 grade), washed with de-ionized water, and rubbed with a smooth polishing cloth to obtain mirror finish. Then it was bathed carefully with triple distilled water and moved rapidly to the corrosion electrolyte (the electrochemical cell).

The different electrochemical experiments have been fulfilled during static conditions at 25 °C in aqueous sulfuric electrolyte, where triply distilled water and analytical grade reagents have been utilized. The electrolyte solution was a stagnant naturally aerated H_2SO_4 solution. Tricine compound was used as an inhibitor purchased from Sigma–Aldrich, and tricine was used without any further purification. The chemical structure of the tricine inhibitor is displayed in Fig. 1.

Different electrochemical measurements were accomplished in a conventional cell of three electrodes, where the carbon steel was used as the working electrode, a Pt rod was the counter electrode, and the reference electrode was saturated calomel electrode (SCE). Before each measurement, the carbon steel sample must be immersed in the corrosive electrolyte at open circuit potential (OCP) for 60 min in order to attain a stable state.

The polarization and EIS experiments have been instigated through the Voltalab PGZ 100 potentiostat/Galvanostat system "*All-in-one*." The cell potentials have been measured versus the saturated calomel electrode, referred to as SCE (0.245 V vs. NHE). All potentiodynamic polarization measurements were operated using a scan rate of 10 mV s^{-1}. The impedance, Z, and phase shift, θ, were recorded in the frequency domain 0.1–10^5 Hz. The sinusoidal potential perturbation was the 10 mV peak-to-peak amplitude. To attain reproducibility, each experiment has been realized at least twice. Details of experimental processes have been explained elsewhere [11, 12]. Corrosion rates, corrosion current density, and hence inhibition efficiencies have been determined via potentiodynamic polarization measurements.

Moreover, the surface morphology of the carbon steel specimens was studied using the Scanning Electron Microscope (SEM) Model Quanta 250 FEG (Field Emission Gun) attached with EDX Unit, with quickening voltage 30 KV, magnification × 14 up to 1,000,000, and resolution for Gun.1n. The carbon steel specimens were examined with and

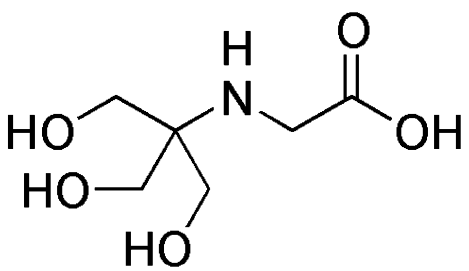

Fig. 1 Chemical structure of tricine inhibitor

without tricine in H_2SO_4 medium after 12-h exposure. The coupons were immersed for 12 h in the blank solution (0.1 M H_2SO_4) without and with 10 mM of tricine at 25 ± 1 °C, washed with distilled water, and then dried in warm air, and finally SEM surface examination was performed.

Quantum chemical studies of the investigated inhibitor have been calculated via the program package 3-21 G** basis set with Hyperchem 7.5 with the semiempirical AM1 procedure for calculating the physical properties of molecules to enhance the experimental data. In fact, many studies have found relations concerning the inhibitor efficiency and quantum mechanical calculations. The tested compound is geometrically optimized with density functional theory (DFT). The theoretical parameters such as the lowest unoccupied molecular orbital energy (E_{LUMO}), the highest occupied molecular orbital energy (E_{HOMO}), energy gap ($\Delta E_{L-H} = E_{LUMO} - E_{HOMO}$), hardness ($\eta$), electronegativity ($X$), dipole moment ($\mu$), fraction of the electron transfer (ΔN), and softness (σ) = $1/\eta$ were calculated for the investigated inhibitor to illuminate the mechanism of the electron transfer among the inhibitor molecules and the carbon steel surface.

3 Results and Discussion

3.1 Potentiodynamic Polarization Measurements

3.1.1 Effect of Inhibitor Concentration

The corrosion behavior of the carbon steel electrode was scrutinized by the polarization technique via Tafel line extrapolation. The potentiodynamic polarization was carried out to determine the effect of the investigated inhibitor on the anodic dissolution of the carbon steel and cathodic reduction reactions. In these measurements, the effect of tricine concentration on the corrosion behavior of the carbon steel electrode in 0.1 M H_2SO_4 acid was investigated. In this respect, the polarization profile of the electrode was recorded in solutions with different concentrations of tricine and presented in Fig. 2. The shape of these curves is very similar either in the anodic or in the cathodic branch, indicating that the mechanisms for both steel dissolution and hydrogen ion reduction nearly remain unchanged after the addition of tricine compound. In acid medium, anodic metal corrosion involves dissolution of metal and the escaping of ions from the surface of metal into the electrolyte, and the cathodic process involves the discharge of H^+ ions to produce H_2 gas. The tested inhibitor may affect either or both the anodic and cathodic processes. The addition of tricine molecules into the corrosive media decreases the current density of the anodic and cathodic processes. This means that the presence of tricine molecules in H_2SO_4 solution inhibits both the hydrogen evolution ($2H^+ + 2e^- \rightarrow H_2$) and the metal dissolution processes ($Fe \rightarrow Fe^{++} + 2e^-$) with displacement of E_{corr} in the direction of more negative values relative to the blank. The calculated numerical values of the change for corrosion potential, E_{corr}, corrosion current density, i_{corr}, cathodic, β_c, and anodic, β_a, Tafel slopes, surface coverage, θ, and the corresponding inhibition efficiency, η %, were derived at different tricine concentrations and are listed in Table 1. These various values were derived via the extrapolating the anodic and cathodic Tafel lines for the potentiodynamic polarization diagram at E_{corr}. The different results depicted in Table 1 and *inst* Fig. 2 suggest that compared to the blank solution, the values of i_{corr} were significantly decreased in the existence of different concentrations of tricine. The decrease of i_{corr} values via increase tricine inhibitor concentration is attributed

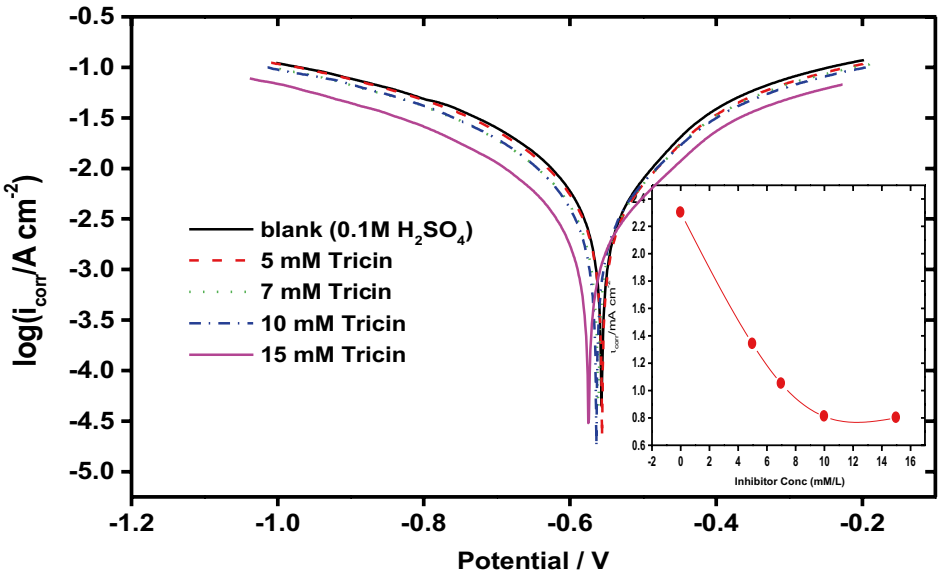

Fig. 2 Potentiodynamic polarization curves of carbon steel electrode in 0.1 M H_2SO_4 solution containing tricine of different concentrations, at 298 K

Table 1 The different corrosion parameters for carbon steel electrode in the absence and addition of different concentrations of tricine at 298 K

Concn. (mM)	E_{corr} ($mV_{(SCE)}$)	i_{corr} (mA cm^{-2})	β_a (mV dec^{-1})	β_c (mV dec^{-1})	θ	η %
0	−553	2.3	107.6	−105.2	–	–
5	−552	1.34	71.2	−69.3	0.417	41.7
7	−557	1.05	63.6	−60.9	0.543	54.3
10	−560	0.81	55.1	−64.9	0.648	64.8
15	−570	0.80	78.5	−80.1	0.652	65.2

to the formation of a protective film between metal surface/electrolyte interfaces through adsorption process. This is also reflected on the values of both anodic Tafel slope (β_a) and cathodic Tafel slope (β_c) in most cases which can be noticed in Table 1. This signifies that both the cathodic and anodic reaction rates have been decreased by the addition of tricine molecules.

The general shift of the E_{corr} in the negative direction and the decrease of the corresponding current densities are due to enlarging the concentration of the tricine inhibitor which increases the inhibitor adsorption on the surface of carbon steel to hinder the direct contact between the carbon steel surface and sulphuric acid electrolyte. The chemical inhibitor compounds can be classified into the anodic or cathodic type inhibitors when the change of E_{corr} is larger than 85 mV with regard to the E_{corr} of blank solution, and if the change of E_{corr} is lower than 85 mV [13]; therefore, the tricine inhibitor can be identified as the mixed type. In the present work, the largest displacement exhibited by tricine is 17 mV (see Table 1), and it may be concluded that this compound acted as a mixed type inhibitor, meaning that the addition of tricine to the 0.1 M H_2SO_4 electrolyte decreased the anodic dissolution of the carbon steel and retarded the cathodic reaction of H_2 generation and can work as a physical barrier to prevent diffusion of the corrosive species into the exposed surface of the carbon steel. The percentage of inhibition efficiency ($\eta\ \% = \theta \times 100$) being the degree of the surface coverage is calculated by [14] $\theta = \left[1 - \frac{i_{corr}}{i^0_{corr}}\right]$, where i_{corr} and i^0_{corr} were the calculated current densities with and without investigated inhibitor. Results of the inhibition efficiencies revealed the good inhibiting action of tricine.

3.1.2 Synergism Consideration

The protection efficiency may increase, decrease, or not affected when two inhibitors molecules were added to each other. When the overall action of inhibitors is greater than the effect of each one individually, this is synergistic inhibition effect. The potentiodynamic polarization curves of carbon steel in 0.1 M H_2SO_4 + 10 mM tricine containing different concentrations of KI at 298 K are presented in Fig. 3. The synergism parameter (***S***) was calculated using the following equation: $S = \frac{1-(\eta_1+\eta_2)}{1-\eta_{1+2}}$,, where η_1 is inhibition efficiency of iodide, η_2 is the inhibition efficiency of tricine, and η_{1+2} is inhibition efficiency of mixture iodide and tricine. The value of ***S*** is calculated at 10 mM tricine + 10 mM KI as 7.9 which is greater than unity implying that the augmented inhibition efficiency is because of synergistic effect of iodide [15, 16].

The data obtained by polarization parameters in the absence and addition of different concentrations of KI to

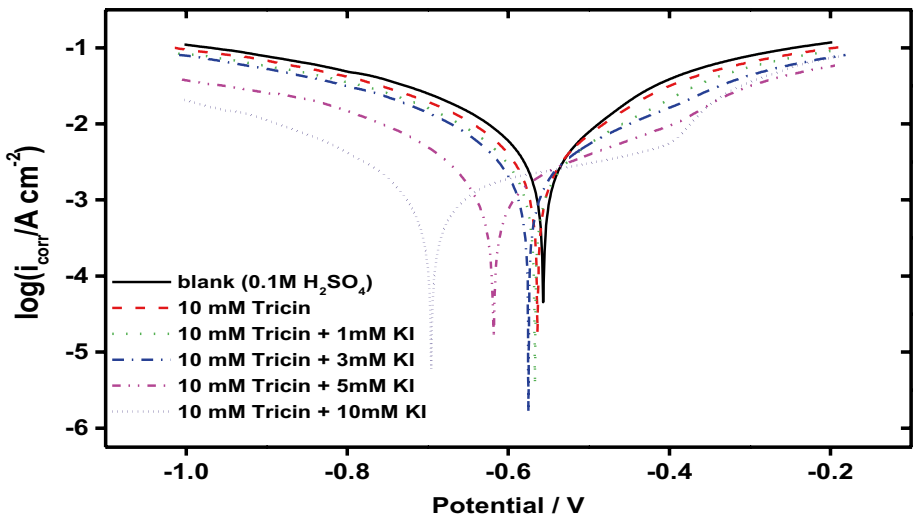

Fig. 3 Potentiodynamic polarization curves of carbon steel in 0.1 M H_2SO_4 + 10 mM tricine containing different concentrations of KI at 298 K

Table 2 Polarization parameters of carbon steel in the absence and presence of different concentrations of *KI* in 10 mM of tricine in aerated stagnant 0.1 M H_2SO_4

Concn KI (mM)	E_{corr} ($mV_{(SCE)}$)	i_{corr} (mA cm^{-2})	β_a (mV dec^{-1})	β_c (mV dec^{-1})	Θ	η %
0	−560	0.81	55.1	−64.9	0.648	64.8
1	−563	0.74	58.0	−66.7	0.678	67.8
3	−571	0.70	58.8	−66.7	0.696	69.6
5	−614	0.50	83.7	−73.4	0.783	78.3
10	−692	0.29	63.6	−66.6	0.874	87.4

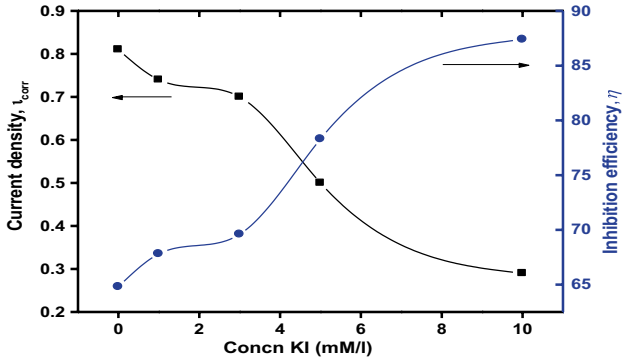

Fig. 4 The corrosion current density, i_{corr}, and the inhibition efficiency η % for carbon steel in 0.1 M H_2SO_4 containing 10 mM tricine with different concentrations of KI

10 mM of tricine + 0.1 M H_2SO_4 at 298 K are showed in Table 2 and Fig. 4. The gradual increase of the KI concentration slightly changed the slopes of Tafel lines for the anodic and the cathodic (β_a and β_c). This assures that there is no variation in the mechanism of inhibition by addition of KI to tricine solutions. The fact that the values of β_c are faintly higher than β_a recommends a cathodic action of the inhibitor. This means that KI is a mixed type inhibitor, but the cathode reaction is more preferentially polarized than the anode. The greater Tafel slope values are due to the surface kinetic process instead of a diffusion-controlled process [17]. Figure 4 shows a variation between the current densities obtained from potentiodynamic polarization curves and the inhibition efficiency with KI concentration in 0.1 M H_2SO_4 + 10 mM tricine solution. It is clear that the presence of I^- ions decreases i_{corr} values and increases the inhibition efficiencies than the presence of 10 mM of tricine in the acid solution.

3.2 The Electrochemical Impedance Measurements, EIS

EIS method provides the information about the corrosion and corrosion inhibition processes and determines the properties of the electrode surface and the kinetics of the electrode processes. There are two types of impedance spectra measured for carbon steel obtained in 0.1 M H_2SO_4 solution in the absence and addition of various concentrations of tricine. One is Nyquist spectrums shown in Fig. 5a and another one is Bode spectrums shown in Fig. 5b. It is obvious from Fig. 5a that the Nyquist plot contained only one single semicircle in high-frequency region and one time

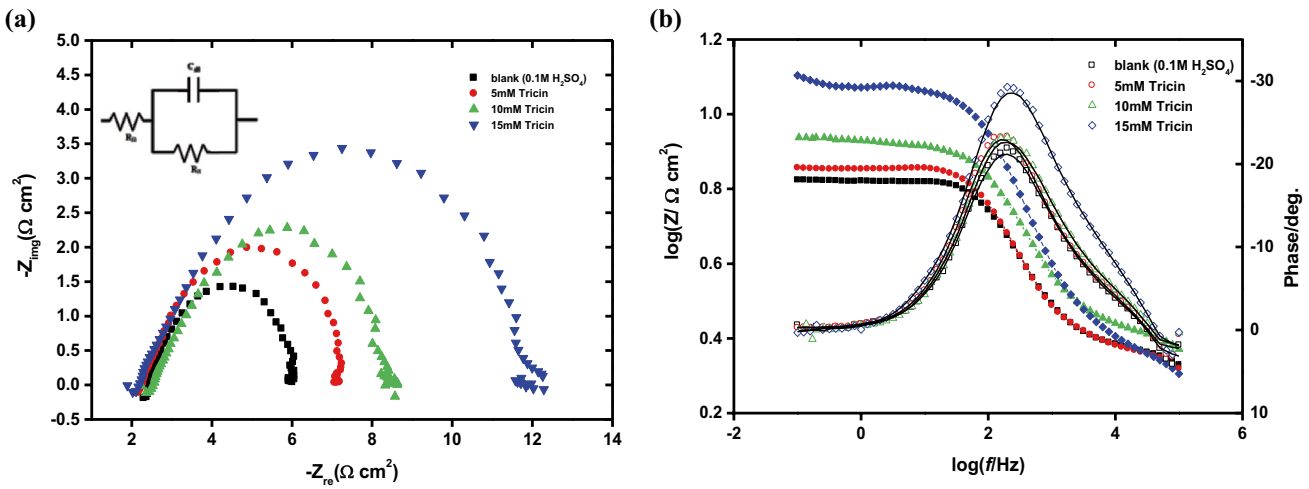

Fig. 5 EIS of carbon steel in 0.1 M H_2SO_4 solution without and with various concentrations of tricine: **a** Bode plots; and **b** Nyquist plots at 298 K

constant appears in Bode plots (*cf.* Fig. 5b) indicating that the process of the charge transfer happens at the electrode/electrolyte interface, and the process of the charge transfer manipulates the corrosion reaction of carbon steel and the addition of the inhibitor has no effect on the mechanism of the carbon steel dissolution [18]. The total impedance and the diameter of the semicircle expanded with increase of the inhibitor concentration which indicates the adsorption of the tricine molecules on the carbon steel surface. Several impedance parameters specifically solution resistance (R_s), resistance of the charge transfer (R_{ct}), and capacitance of the double layer (C_{dl}) were calculated using equivalent circuit exhibited in *inst* Fig. 5a and are listed in Table 3. From Table 3, it is observed that the values of R_{ct} significantly increase with the addition of tricine inhibitor compared with the blank solution. An increase in R_{ct} values is on account of the formation of protecting film at the carbon steel/solution interface.

Figure 6 displays the Nyquist and Bode plots of carbon steel electrode after immersion in 0.1 M H_2SO_4 and 10.0 mM tricine solution without and with different concentrations of I^- ions. The Nyquist plots showed only one capacitive loop in high-frequency region, and the diameter increases as the KI concentration increases. In presence of KI, the diameter of Nyquist plot is higher than the other two cases. This behavior indicates that tricine molecules adsorb on the carbon steel surface and form a protective layer, which decelerates the dissolution process, and the largest effect is obtained with the addition of tricine/KI mixture. This explains that I^- ion increases the inhibition efficiency of tricine, which is in a good agreement with the data obtained by potentiodynamic polarization measurements. Bode plot shows simply one time constant and the phase maxima increases as the concentration of KI increases reaching to its maximum value at 10 mM KI (Table 4).

3.3 Adsorption Isotherm Studies

To understand the mechanism of tricine adsorption at the carbon steel surface, the adsorption isotherm was also studied. In acidic media, the corrosion inhibition process occurs by appropriate adsorption of tested inhibitor molecules at

Table 3 Equivalent circuit parameters of carbon steel electrode in the absence and addition of different concentrations of tricine in naturally aerated stagnant 0.1 M H_2SO_4 at 298 K

Conc. (ppm)	R_s (Ω)	R_{ct} (Ω cm^2)	C_{dl} (μF cm^{-2})	α
0	2.3	4.7	269	0.98
5	2.3	5.2	307	0.98
7	2.2	6.1	260	0.98
10	2.6	6.3	253	0.98
15	2.2	10.4	153	0.99

Table 4 Equivalent circuit parameters of carbon steel electrode in the absence and addition of different concentrations of KI in naturally aerated stagnant 0.1 M H_2SO_4 + 10 mM tricine at 298 K

Conc. (ppm)	R_s (Ω)	R_{ct} (Ω cm^2)	C_{dl} (μF cm^{-2})	α
0	2.6	6.3	253	0.98
1	2.7	8.4	301	0.98
3	2.3	9.0	279	0.98
5	2.8	27.5	183	0.99
10	2.5	65.1	154	0.99

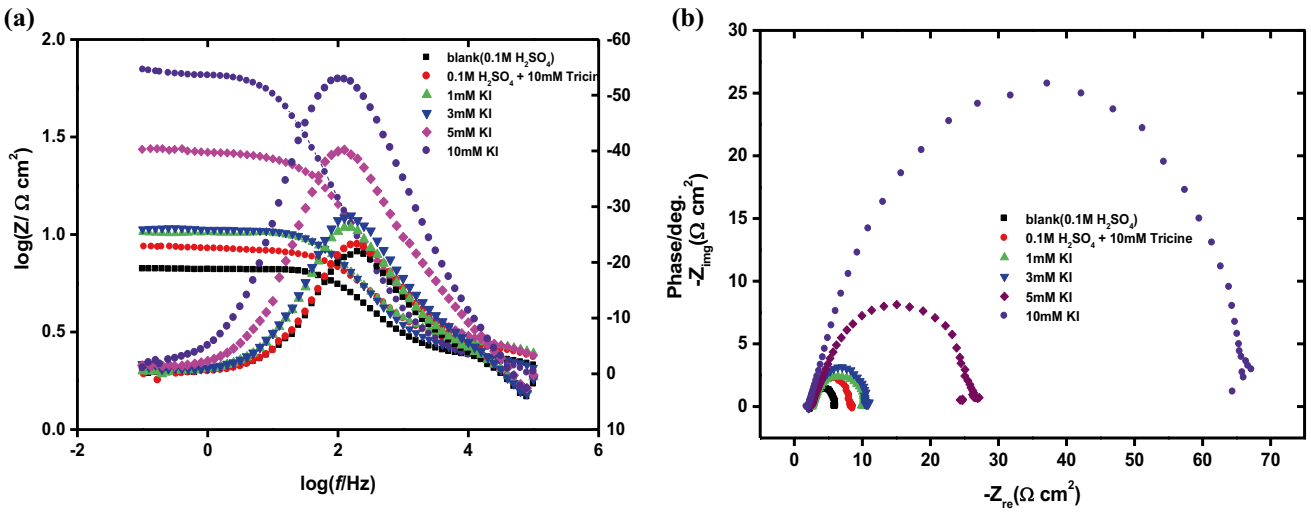

Fig. 6 Electrochemical impedance spectra of carbon steel after immersion in 0.1 M H_2SO_4 + 10.0 mM tricine solutions without and with KI at various concentrations: **a** Bode plots; and **b** Nyquist plots at 298 K

the metal/solution interface. Generally, the adsorption phenomena happen as a consequence of the electrostatic attraction between (i) metal ions and the atoms with lone pairs of electrons such as *N* hold by tricine inhibitor, (ii) the polar interaction between uncharged inhibitor molecules with the metal, (iii) interaction of the type π with the metal, and (IV) all of the previous [19]. The adsorption process is based on the electronic structure of the inhibitor, the nature of metal surface, reaction temperature, and the number of active centers on the metal surface [20]. In order to specify the adsorption mode of tricine molecules on the steel electrode surface in H_2SO_4 electrolyte, the degree of surface coverage, θ, at different concentrations of the investigated inhibitor in 0.1 M H_2SO_4 electrolyte was determined from the corresponding electrochemical polarization measurements. The values of surface coverage θ have been fitted to determine the type of adsorption isotherm with Temkin, Frumkin, Freundlich, and Langmuir isotherms. The appropriate match is realized to conform with the Langmuir adsorption isotherm which depends on the hypothesis that all adsorption sites are equal and particle binding happens separately from adjacent sites being occupied or not [21]: $KC = \frac{\theta}{1-\theta}$, where C is the concentration of tricine inhibitor, K symbolizes the adsorption equilibrium constant correlated to the free energy of adsorption ΔG_{ads} as [22] $K = \frac{1}{C_{solvent}} \exp(-\Delta G/RT)$, and θ is the fractional surface coverage, where $C_{solvent}$ acts as the molar concentration of a solvent. In the case of water, $C_{solvent}$ is 55.5 mol dm^{-3}, R implies the universal gas constant, and T signifies the absolute temperature. The above equation $\left(KC = \frac{\theta}{1-\theta}\right)$ can be reordered to acquire the following formulation: $\frac{C}{\theta} = \frac{1}{K} + C$. A plot of C/θ as a function of C gives a straight line with a slope of unity. This linear relationship has been confirmed for the adsorption of tricine on the surface of carbon steel (*cf.* Figure 7). The free energy of adsorption, ΔG_{ads}, was calculated and found to be equal to -32.6 kJ mol^{-1} in case of tricine and -37.5 kJ mol^{-1} in case of tricine + KI. A value of -40 kJ mol^{-1} is usually adopted as a threshold value between chemi- and physisorption [22]. Therefore, the adsorption of tricine molecules on carbon steel electrode is of a physical nature. The value of ΔG_{ads} in the presence of KI is higher than in case of tricine only indicating higher inhibition efficiency in the presence of KI.

3.4 Inhibition Mechanism

The above data approve that the tricine molecule acted as a good corrosion inhibitor for carbon steel in H_2SO_4 solutions. The corrosion inhibition of tricine is the result of their physical adsorption and formation of protective layer on the carbon steel electrode surface. The pervious investigation illustrated that the carbon steel surface in acid electrolyte is positively charged [23, 24]. Moreover, in aqueous acid solutions, the amino acids exist either as neutral molecules or in the form of cations [25, 26]. Therefore, these amino acids can adsorb into the positively charged metal surface in the form of neutral molecules incorporating the dislodgment of water molecules from the surface of a metal via contribution lone pairs of electrons by N atoms with the metal surface [27]. Furthermore, adsorption can occur via the already adsorbed SO_4^- anions at the positively charged metal surface. The adsorbed SO_4^- anions at the metal surface make a negatively charged double layer and consequently it results in an increase in the adsorption capability of the protonated tricine compounds. Figure 8 displays the schematic representation of adsorption of the tricine molecules over the steel surface via electrostatic attraction.

It is known that the adsorption ability of I^- ions is higher than that of SO_4^{2-} ions. Consequently, I^- ions are also adsorbed at the carbon steel surface in competition with SO_4^{2-} ions, which produce excess surface charge of Fe. This process enhances the adsorption of the positively charged tricine molecules.

3.5 SEM Surface Morphology Studies

Surface morphology of carbon steel electrode was studied by scanning electron microscopy, SEM. Figure 9 presents SEM images obtained on the steel surface before and after dunking in 0.1 M H_2SO_4 with and without the addition of the tricine with 10 mM for 6 h at 298 K. From Fig. 9a, it can be seen that the fresh carbon steel surface was homogenous morphological structure. Nevertheless, after dipping an extreme change of the surface state is observed. In the absence of inhibitor, the surface state was strongly damaged due to some cracks and pits as a result of the attack of corrosive solution (Fig. 9b). In the presence of 10 mM tricine + 10 mM KI in sulfuric acid electrolyte, SEM image of the carbon steel surface is considerably unaffected by corrosive medium as exhibited in Fig. 9c. This indicates that tricine molecules hinder the dissolution of the carbon steel by forming good protective layer adsorbed on the specimen's surface which is responsible for the inhibition of corrosion.

3.6 Quantum Chemical Study of Inhibitor

Various quantum chemical approaches have been performed to associate the geometrical and electronic structures of inhibitors with their inhibition efficiency of the corrosion [28–30]. The activity of the tricine inhibitor is thoroughly accompanying to its frontier molecular orbitals (MO), including highest occupied molecular orbital, *HOMO*, and lowest unoccupied molecular orbital, *LUMO*, and the other parameters such as softness and hardness. The optimized geometry of tricine molecule is shown in Fig. 10. The adsorption of tricine molecule on the carbon steel surface in

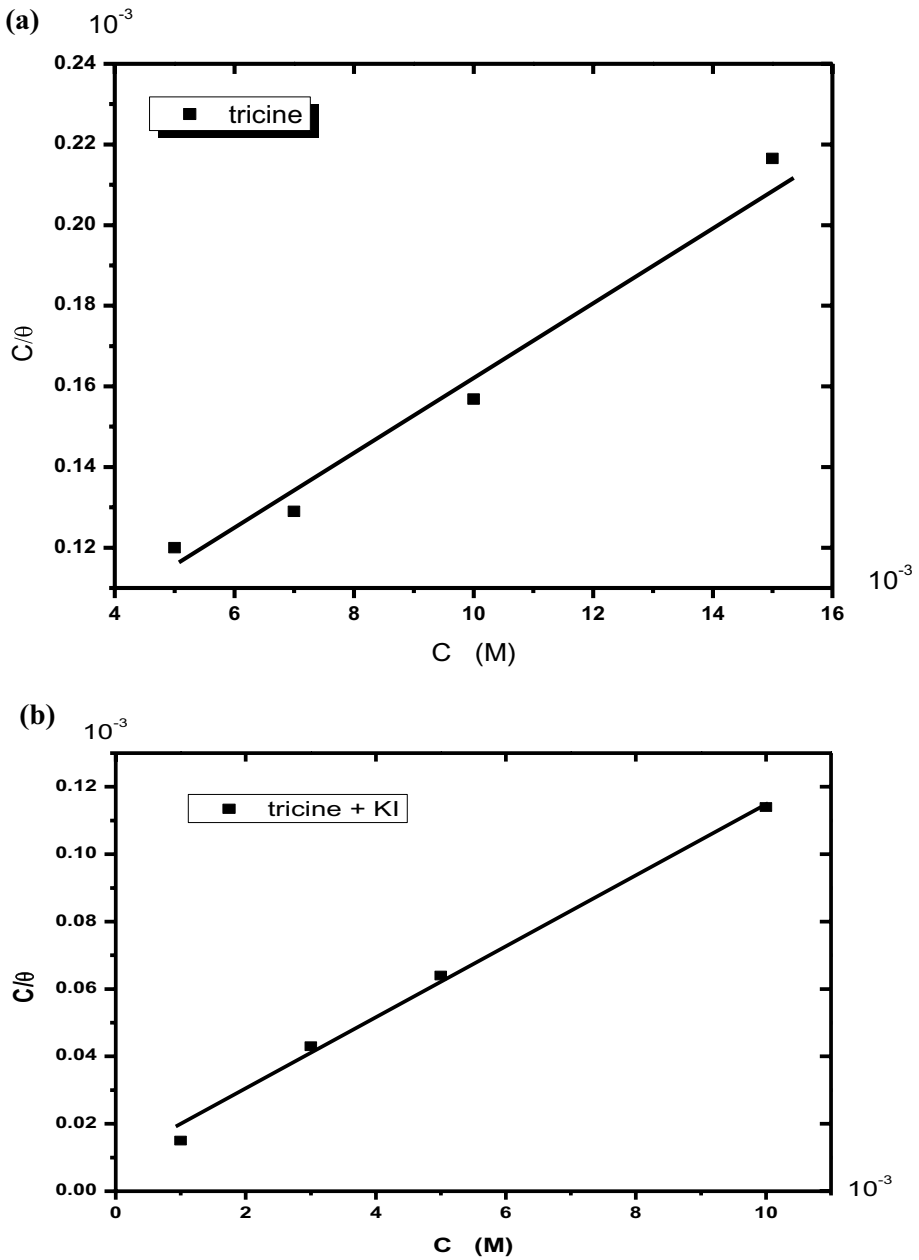

Fig. 7 Langmuir adsorption isotherm of tricine (**a**) and tricine + KI (**b**) on the carbon steel surface in 0.1 M H_2SO_4 at 298 K

acidic solution may be achieved by the interaction between the unshared electron pairs in oxygen with the *d*-orbitals of *Fe* atom. The presence of O and N atoms together in tricine molecule ensures strong adsorption on the Fe electrode surface. The evaluated bond angles and bond length of the tricine inhibitor are presented in Tables 5 and 6. The HOMO and LUMO (Frontier molecular orbitals) of chemical compounds act an essential role in explaining their reactivity and hence adsorption onto the surface of carbon steel takes place. The *3d*-unfilled Fe ([Ar] $4s^2$ $3d^6$) orbital could bond with the highest occupied molecular orbital (*HOMO*) of tricine, while the filled *4s* orbital could interact with the lowest unoccupied molecular orbital (*LUMO*) of the tricine molecules [31]. The electronic orbital density distributions of *HOMO* and *LUMO* for tricine molecule are displayed in Fig. 11a, b. The frontier molecular orbital theory confirms the chemical activity resulted from the interaction involving levels of *LUMO* and *HOMO* for the reacting species [30].

The E_{HOMO} and E_{LUMO} provide information about the reactivity of the tested compounds. E_{HOMO} is a quantum chemical parameter which is usually linked with the electron contributing ability of the molecule. The high value of E_{HOMO} provides the ability of the molecule to share the electrons to proper acceptor molecule which has the low empty molecular orbital [32]. Therefore, E_{LUMO} entails the ability of the inhibitor's molecule to accept the electrons

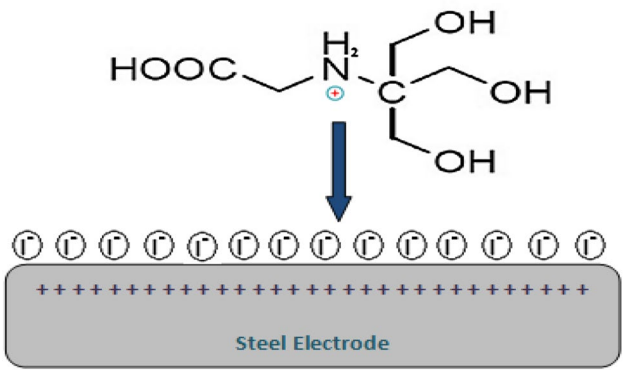

Fig. 8 Suggested model of adsorption of the tricine inhibitor on steel electrode

from an electron-rich species, which implies that the inhibition efficiency of tested inhibitor is expected to increase with decreasing values of E_{LUMO} [33].

Therefore, an increase in the value of E_{HOMO} can facilitate the adsorption of inhibitor molecules by increasing its capability to give electrons to the appropriate acceptor leading to better adsorption, and therefore better corrosion inhibition efficiency is achieved. The energy gap ΔE ($E_{LUMO} - E_{HOMO}$) should be small for an inhibitor for good interaction with metal surface. In fact, the efficiency of the inhibitor boosts via the lower dipole moments, diminishing molecular size and augmenting nitrogen charge [32, 34, 35]. Table 7 shows the calculated quantum chemical properties for tricine molecule in aqueous phase, E_{HOMO} (eV), E_{LUMO} (eV), dipole moment, μ (D), and the total energy. Quantum chemical parameters listed in Table 7 reveal that tricine has the highest E_{HOMO} and low E_{LUMO} with high energy gap which enhance the assumption that tricine will adsorb more strongly on the carbon steel surface and this can happen depending on the donor–acceptor interactions between the inhibitor molecules and the empty *d*-orbitals of the metal surface [36]. The negative sign of the E_{HOMO} indicates that the adsorption is physisorption which confirms the data obtained by adsorption isotherm studies [37]. Figure 12 exhibits the molecular orbital distribution of tricine molecules. The displayed data in Tables 7 and 8 show that

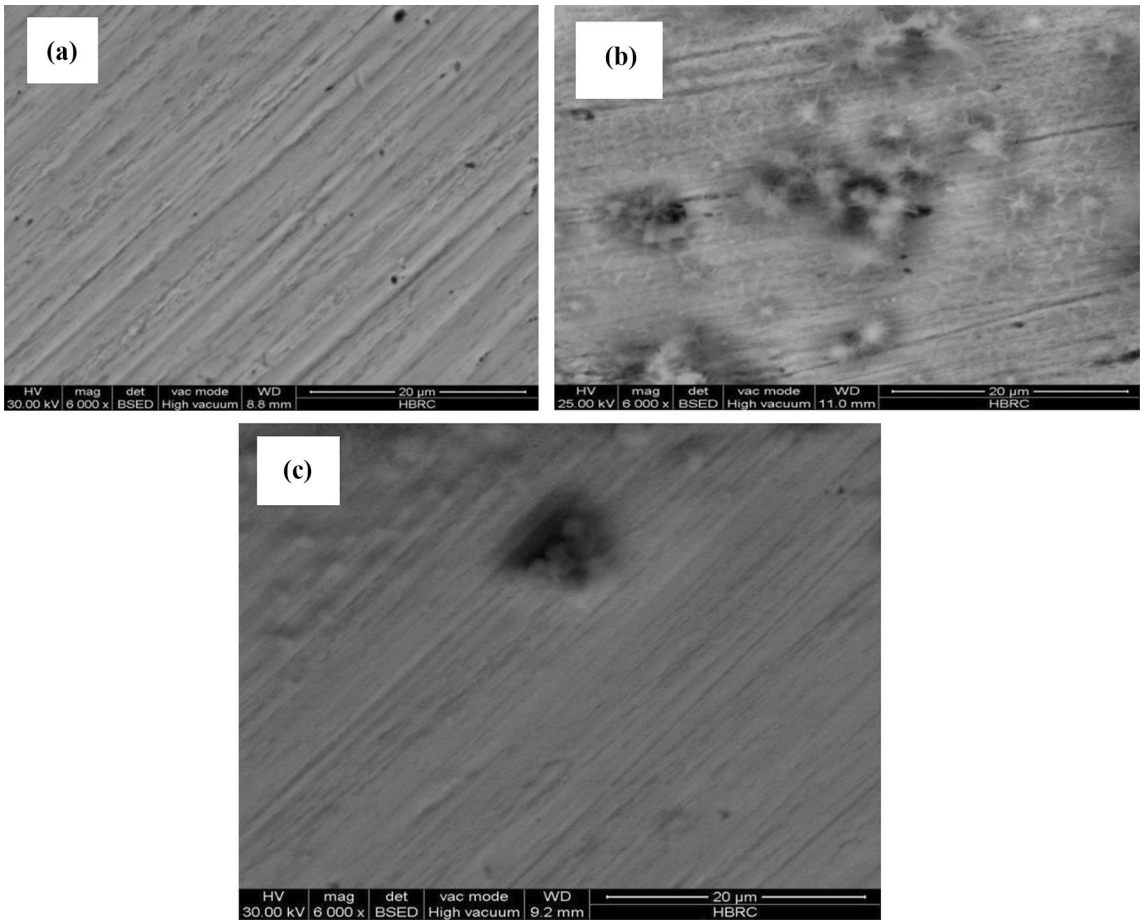

Fig. 9 SEM micrographs of carbon steel after 6 h at 298 K in 0.1 M H_2SO_4 in the absence and addition of investigated inhibitor. **a** polished sample, **b** 0.1 M H_2SO_4, **c** 0.1 M H_2SO_4 + 10 mM tricine + 10 mM KI

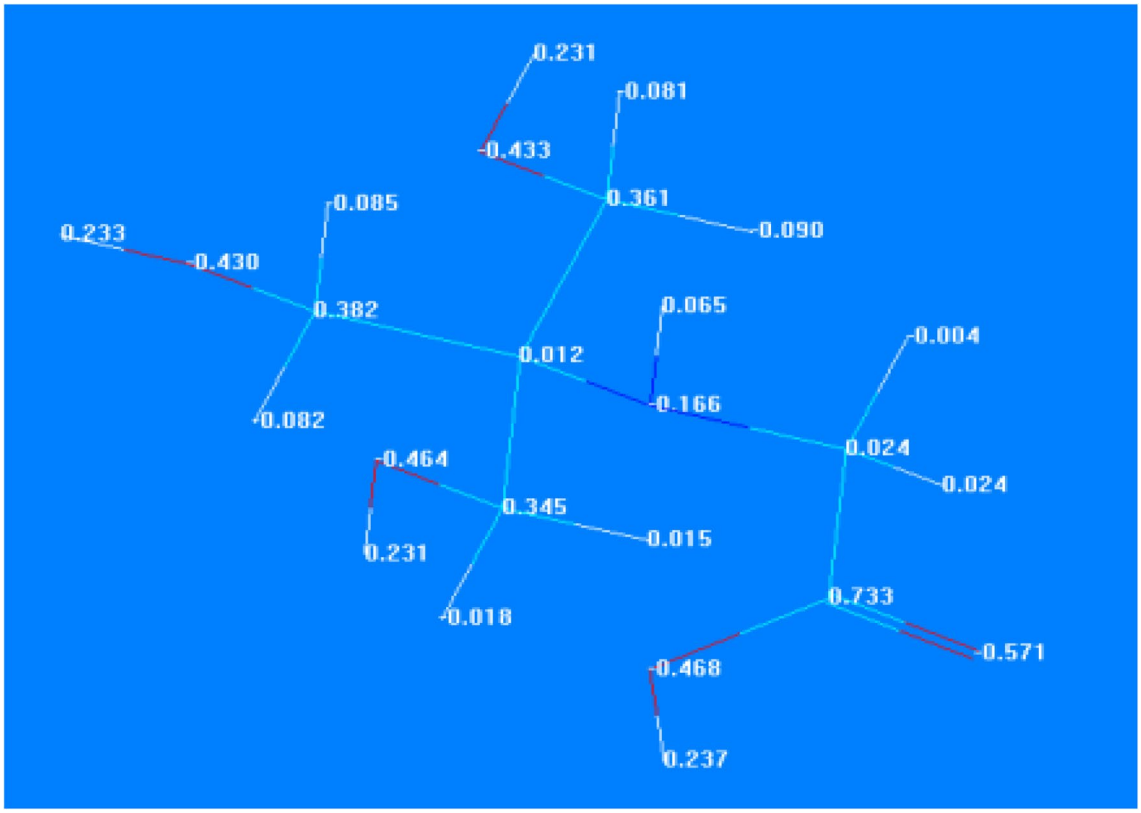

Fig. 10 Optimized molecular structure of tricine molecule

Table 5 Selected bond lengths of tricine compound

	Type	Start atom	End atom	Bond order	Rotatable	Length /Angstrom
Bond 1	N–H	N	H1	1	No	1.02115
Bond 2	N–C	N	C1	1	Yes	1.47466
Bond 3	C–C	C1	C2	1	No	1.5205
Bond 4	C–O	C2	O1	2	No	1.21226
Bond 5	C–O	C2	O2	1	No	1.35053
Bond 6	N–C	N	C3	1	Yes	1.50998
Bond 7	C–C	C3	C4	1	Yes	1.55905
Bond 8	C–O	C4	O3	1	No	1.4237
Bond 9	C–C	C3	C5	1	Yes	1.56237
Bond 10	C–O	C5	O4	1	No	1.42056
Bond 11	C–C	C3	C6	1	Yes	1.57165
Bond 12	C–O	C6	O5	1	No	1.41988
Bond 13	C–H	C1	H2	1	No	1.09684
Bond 14	C–H	C1	H3	1	No	1.09237
Bond 15	O–H	O2	H4	1	No	0.978736
Bond 16	C–H	C4	H5	1	No	1.09519
Bond 17	C–H	C4	H6	1	No	1.09623
Bond 18	O–H	O3	H7	1	No	0.972803
Bond 19	C–H	C5	H8	1	No	1.09325
Bond 20	C–H	C5	H9	1	No	1.09643
Bond 21	O–H	O4	H10	1	No	0.971655
Bond 22	C–H	C6	H11	1	No	1.09623

Table 6 Selected angles of tricine compound

	Type	Start atom	Vertex	End atom	Angle (°)
Angle 1	HNC	H1	N	C1	107.1412
Angle 2	HNC	H1	N	C3	107.9058
Angle 3	CNC	C1	N	C3	118.9223
Angle 4	NCC	N	C1	C2	115.3358
Angle 5	NCH	N	C1	H2	107.6572
Angle 6	NCH	N	C1	H3	112.1560
Angle 7	CCH	C2	C1	H2	105.66643
Angle 8	CCH	C2	C1	H3	109.3899
Angle 9	HCH	H2	C1	H3	105.9982
Angle 10	CCO	C1	C2	O1	125.4669
Angle 11	CCO	C1	C2	O2	114.1655
Angle 12	OCO	O1	C2	O2	120.2951
Angle 13	COH	C2	O2	H4	104.2372
Angle 14	NCC	N	C3	C4	110.6082
Angle 15	NCC	N	C3	C5	111.4074
Angle 16	NCC	N	C3	C6	103.7585
Angle 17	CCC	C4	C3	C5	111.0063
Angle 18	CCC	C4	C3	C6	109.4848
Angle 19	CCC	C5	C3	C6	110.3388
Angle 20	CCO	C3	C4	O3	114.8745
Angle 21	CCH	C3	C4	H5	109.8763
Angle 22	CCH	C3	C4	H6	110.3379

tricine in the protonated structure has the lowest hardness; this agrees with the experimental results that tricine attains high inhibitive influence on the carbon steel surface via the protonated structure, i.e., through electrostatic interaction between the cation form of tricine and the vacant *d*-orbital of steel.

The dipole moment is the important electronic parameter which is originated from a variable charge distribution on the different atoms of the molecule. It is primarily utilized to investigate the intermolecular interactions including the Vander Waals type dipole–dipole forces, because the larger the dipole moment, the stronger will be the intermolecular attraction [38]. The significant value of dipole moment boosts possibly the adsorption between the metal surface and chemical compound [39].

Molecular modeling calculations also allow the investigation of the particularly stable adsorption configurations of the tricine inhibitor molecule. The side and top views of the lowest adsorption configurations of tricine molecule on carbon steel surface are shown in Fig. 13. The quantum chemical calculations showed that the molecule belonging to the set 1, Fig. 13, adsorb nearly parallel on carbon steel surface. This adsorption configuration instigated from the distribution of LUMO and HOMO densities by entire tricine molecules, which proposes that the adsorption of tricine molecule on the carbon steel surface occurs via the electron-donation route and the electron-back donation mechanism. In addition, from the top views it is noticed the polarizable atoms favorably occupied the vacant positions, appearing to escape the atoms on the

Table 7 Quantum chemical parameters of the tricine inhibitor

E_{HOMO} (eV)	E_{LUMO} (eV)	ΔE (eV)	μ (Debye)	Log P	ΔN (eV)
− 8.375	0.975	9.35	2.521	2.191	0.352

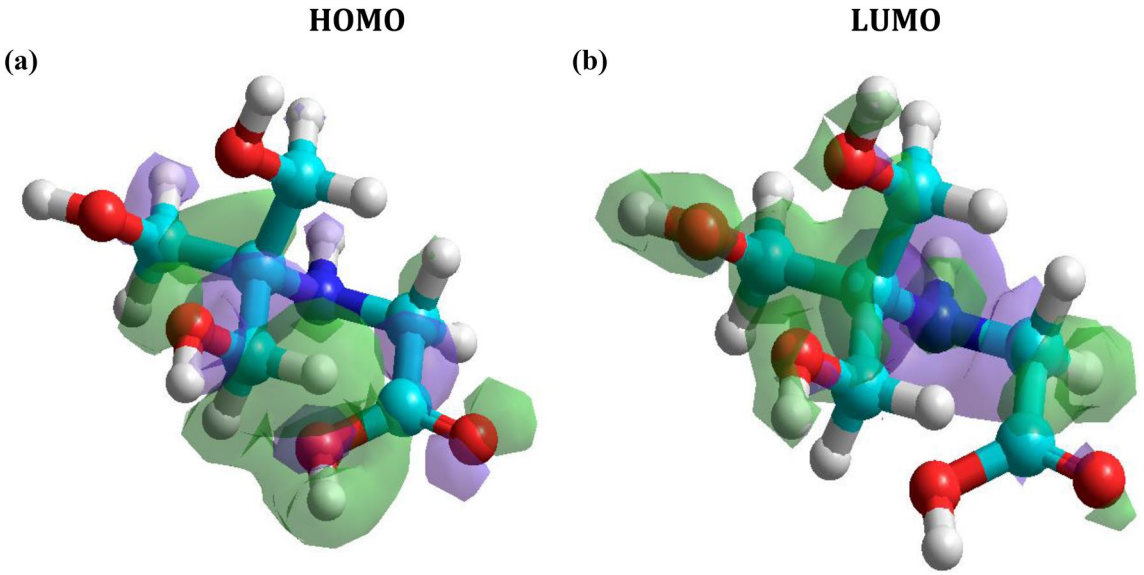

Fig. 11 The frontier molecular orbital of studied tricine molecular: **a** HOMO, **b** LUMO

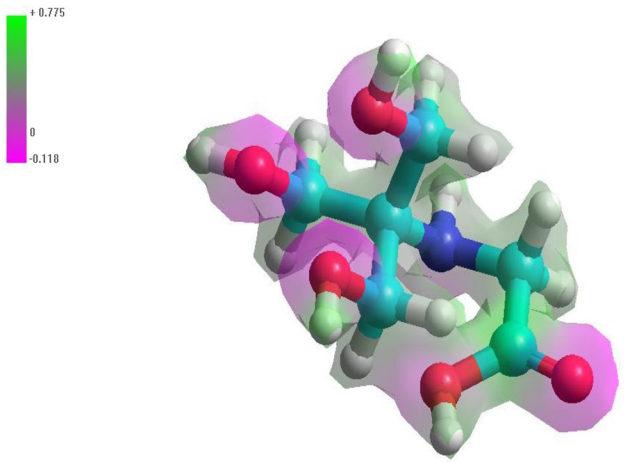

Fig. 12 3D molecular electrostatic potential map of the tricine molecule

Table 8 Other calculated quantum chemical parameters of the investigated inhibitor

Ionization potential, I (eV)	Electron affinity, A (eV)	Electron-egativity (eV mol^{-1})	Global hardness (eV mol^{-1})	Softness, $\sigma = 1/\eta_{inh}(eV^{-1})$
8.375	−0.975	3.7	4.675	0.213904

corresponding surface planes. This analysis is in a good agreement alongside Heinz et al. [40], illustrating a similar accommodation of the peptides molecules on a gold, palladium, and Pd–Au surfaces.

4 Conclusion

From the experimental results of the present work, we can conclude the following:

- Tricine mainly acts as good mixed inhibitor for the corrosion of carbon steel in 0.1 M H_2SO_4.
- Inhibition efficiency increases with an increase in the concentration of the tricine.
- A good agreement is obtained for the inhibition efficiency determined by EIS and polarization methods.
- The SEM image of the surface morphology assures the formation of layer of tricine formed on the carbon steel.
- Addition of iodide greatly helps tricine to higher corrosion inhibition of carbon steel in sulfuric acid.
- The adsorption of tricine on the mild steel surface obeys the Langmuir isotherm model.
- The theoretical and experimental data confirm that the inhibition efficiency of tricine in acidic electrolyte depends on physical adsorption of the tricine molecules.

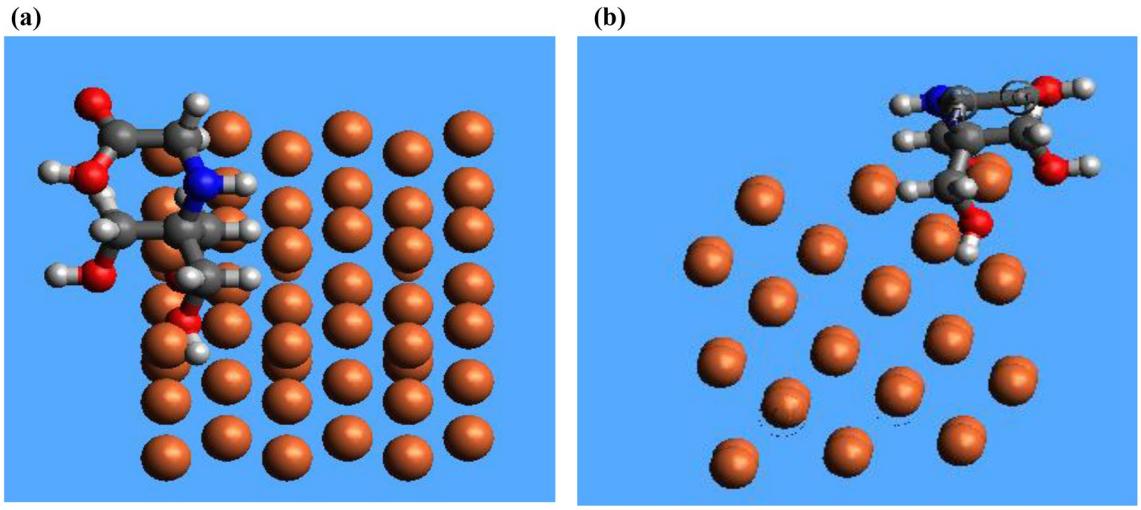

Fig. 13 Equilibrium adsorption configurations performed for tricine on Fe surface in aqueous solution. **a** side view, **b** top view

References

1. Hashem N, Negem M (2016) Ni-Cu nano-crystalline alloys for efficient electrochemical hydrogen production in acid water. RSC Adv 6:51111e9
2. Nady H, Negem M (2018) Electroplated Zn–Ni nanocrystalline alloys as an efficient electrocatalyst cathode for the generation of hydrogen fuel in acid medium. Int J Hydrogen Energy 43:4942–4950
3. Negem M, Hashem N (2017) Electroplated Ni-Cu nanocrystalline alloys and their electrocatalytic activity for hydrogen generation using alkaline solutions. Int J Hydrogen Energy 42:28386–28396
4. Negem M, Nady H, El-Rabiei MM (2019) Nanocrystalline nickel–cobalt electrocatalysts to generate hydrogen using alkaline solutions as storage fuel for the renewable energy. Int J Hydrogen Energy 44:11411–11420
5. Ramesh S, Rajeswari S, Maruthamuthu S (2003) Effect of inhibitors and biocide on corrosion control of mild steel in natural aqueous environment. Mater Lett 57:4547
6. Eddy NO, Ebenso EE (2008) Corrosion inhibitive properties and adsorption behaviour of ethanol extract of Piper guinensis as a green corrosion inhibitor for mild steel in H2SO4. Afr J Pure Appl Chem 2:107
7. Eddy NO, Odoemelam SA (2009) Corrosion inhibition and adsorption properties of ethanol extract of Gongronema latifolium on mild steel in H2SO4. Pigment Resin Technol 38:111
8. Jeyaprabha C, Sathiyanarayanan S, Venkatachari G (2006) Influence of halide ions on the adsorption of diphenylamine on iron in 0.5 M H2SO4 solutions. Electrochim Acta 51:4080
9. Harek Y, Larabi L (2004) Corrosion inhibition of mild steel in 1 mol dm^3 HCl by oxalic N-phenylhydrazide N-Phenylthiosemicarbazide. Kem. Ind 53(2):55
10. El-Feky HE, Helal NH, Negem MR (2010) Electrochemical behavior of some copper alloys in sulfuric acid solutions. Mater Corros 61:599
11. El-Rabiee MM, Helal NH, Abd El-Hafez GhM, Badawy WA (2008) Corrosion control of vanadium in aqueous solutions by amino acids. J Alloys Compd 459:466
12. Badawy WA, Helal NH, El-Rabiee MM, Nady H (2010) Electrochemical behavior of Mg and some Mg alloys in aqueous solutions of different pH. Electrochim Acta 55:1880
13. Li W, He Q, Zhang S, Pei C, Hou B (2008) Some new triazole derivatives as inhibitors for mild steel corrosion in acidic medium. J Appl Electrochem 38:289–295
14. Quartarone G, Battilana M, Bonaldo L, Tortato T (2008) Investigation of the inhibition effect of indole-3-carboxylic acid on the copper corrosion in 0.5 M H_2SO_4. Corros Sci 50:3467
15. Pavithra MK, Venkatesha TV, Vathsala K, Nayana KO (2010) Synergistic effect of halide ions on improving corrosion inhibition behaviour of benzisothiozole-3-piperizine hydrochloride on mild steel in 0.5 M H_2SO_4 medium. Corros Sci 52:3811
16. Umoren SA, Ogbobe O, Igwe IO, Ebenso EE (2008) Inhibition of mild steel corrosion in acidic medium using synthetic and naturally occurring polymers and synergistic halide additives. Corros Sci 50:1998–2006
17. Fouda AS, El-Taib Heakal F, Radwan MS (2009) Role of some thiadiazole derivatives as inhibitors for the corrosion of C-steel in 1 M H_2SO_4. J Appl Electrochem 39:391
18. Amin MA, Khaled KF (2010) Copper corrosion inhibition in O2-saturated H_2SO_4 solutions. Corros Sci 52:1194
19. Schweinsberg D, George G, Nanayakkawa A, Steinert D (1988) The protective action of epoxy resins and curing agents—inhibitive effects on the aqueous acid corrosion of iron and steel. Corros Sci 28:33
20. Abdel-Gaber AM, Abd-El-Nabey BA, Sidahmed IM, El-Zayady AM, Saadawy M (2006) Inhibitive action of some plant extracts on the corrosion of steel in acidic media. Corros Sci 48:2765
21. Popova A, Christov M, Raicheva S, Sokolova E (2004) Adsorption and inhibitive properties of benzimidazole derivatives in acid mild steel corrosion. Corros Sci 46:1333
22. Lipkowski J, Ross PN (eds) (1992) Adsorption of molecules at metal electrodes. VCH, New York
23. Bentiss F, Lebrini M, Vezin H, Chai F, Traisnel M, Lagrené M (2009) Enhanced corrosion resistance of carbon steel in normal sulfuric acid medium by some macrocyclic polyether compounds containing a 1,3,4-thiadiazole moiety: AC impedance and computational studies. Corros Sci 51:2165
24. Solmaz R, Kardas G, Yazc B, Erbil M (2008) Adsorption and corrosion inhibitive properties of 2-amino-5-mercapto-1, 3, 4-thiadiazole on mild steel in hydrochloric acid media. Colloids Surf A 312:7
25. Amin MA, Abd Sayed S, El Rehim TM, Hesham Abdel-Fatah (2009) Electrochemical frequency modulation and inductively coupled plasma atomic emission spectroscopy methods for monitoring corrosion rates and inhibition of low alloy steel corrosion in HCl solutions and a test for validity of the Tafel extrapolation method. Corros Sci 51:882
26. Abdallah M, Megahed HE (1995) Cyclic voltammograms of iron and C-steels in oxalic acid solutions and investigation of the effect of phenyl phthalimide as corrosion inhibitors. Monat Chem 126:519
27. Bentiss F, Traisnel M, Gengembre L, Lagrené M (1999) A new triazole derivative as inhibitor of the acid corrosion of mild steel: electrochemical studies, weight loss determination, SEM and XPS. Appl Surf Sci 152:237
28. Obot IB, Obi-Egbedi NO (2010) Theoretical study of benzimidazole and its derivatives and their potential activity as corrosion inhibitors. Corros Sci 52:657
29. Gao G, Liang C (2007) Electrochemical and DFT studies of β-amino-alcohols as corrosion inhibitors for brass. Electrochim Acta 52:4554
30. Musa AY, Kadhum AH, Mohamad AB, Rohoma AB, Mesmari H (2010) Electrochemical and quantum chemical calculations on 4,4-dimethyloxazolidine-2-thione as inhibitor for mild steel corrosion in hydrochloric acid. J Mol Struct 969:233
31. Li Y, Zhao P, Liang Q, Hou B (2005) Berberine as a natural source inhibitor for mild steel in 1 M H2SO4. Appl Surf Sci 252:1245
32. Gece G, Bilgic S (2009) Quantum chemical study of some cyclic nitrogen compounds as corrosion inhibitors of steel in NaCl media. Corros Sci 51:1876
33. Ahamad I, Prasad R, Quraishi MA (2010) Adsorption and inhibitive properties of some new Mannich bases of Isatin derivatives on corrosion of mild steel in acidic media. Corros Sci 52:1472
34. Yurt A, Ulutas S, Dal H (2006) Electrochemical and theoretical investigation on the corrosion of aluminium in acidic solution containing some Schiff bases. Appl Surf Sci 253:919
35. Chao P, Liang Q, Li Y (2005) Electrochemical, SEM/EDS and quantum chemical study of phthalocyanines as corrosion inhibitors for mild steel in 1 mol/l HCl. Appl Surf Sci 252:1596
36. Hackerman N, Snavely E Jr, Payne JS Jr (1966) Effects of anions on corrosion inhibition by organic compounds. J Appl Electrochem 113:677
37. Gece G (2008) The use of quantum chemical methods in corrosion inhibitor studies. Corros Sci 50:2981
38. Dwivedi A, Misra N (2010) Quantum chemical study of Etodolac (Lodine). Der Pharma Chem 2:58
39. Li X, Deng S, Fu H, Li T (2009) Adsorption and inhibition effect of 6-benzylaminopurine on cold rolled steel in 10 M HCl. Electrochim. Acta 54:4089

40. Heinz H, Farmer BL, Pandey RB, Slocik JM, Patanaik SS, Pachter R, Naik RR (2009) Nature of molecular interactions of peptides with gold, palladium, and Pd−Au bimetal surfaces in aqueous solution. J Am Chem Soc 31:9704